



ELSEVIER

Nuclear Instruments and Methods in Physics Research B 190 (2002) 89–94

NIM B
Beam Interactions
with Materials & Atoms

www.elsevier.com/locate/nimb

Electronic energy loss of swift protons in the oxides Al_2O_3 , SiO_2 and ZrO_2

Isabel Abril ^{a,*}, Rafael Garcia-Molina ^b, Néstor R. Arista ^c,
Carlos F. Sanz-Navarro ^d

^a *Departament de Física Aplicada, Universitat d'Alacant, Apartat 99, E-03080 Alacant, Spain*

^b *Departamento de Física, Universidad de Murcia, Apartado 4021, E-30080 Murcia, Spain*

^c *Instituto Balseiro, Centro Atómico Bariloche, RA-8400 Bariloche, Argentina*

^d *School of Physical and Mathematical Sciences, University of Loughborough, LE11 3TU, UK*

Abstract

We have evaluated the energy loss of protons when moving through several oxides (Al_2O_3 , SiO_2 , and ZrO_2). The calculations were done in the framework of the dielectric formalism, using a combination of Mermin-type energy-loss functions to describe the outer electrons, together with generalized oscillator strengths to take into account electrons from the inner shells. This method provides a realistic description of the electronic properties of each target. The calculated stopping cross-sections compare fairly well with the available experimental data in a wide range of proton energies. © 2002 Elsevier Science B.V. All rights reserved.

PACS: 34.50.Bw; 77.22.-d; 47.27.Vf; 61.46.+w

Keywords: Stopping power; Proton energy loss; Energy-loss straggling; Dielectric properties of solids

The energy loss of ions in elements and chemical compounds is a subject of great interest for basic research and for multiple applications in atomic physics and materials science. In particular, the energy deposition in oxides is a question of special interest due to its multiple technological applications. Previous [1] and more recent [2–4] experiments provide precise determinations of the stopping cross-sections of some insulators, using foil transmission and backscattering techniques, over a wide range of energies. These experiments

allow to study the contribution of valence electrons and to analyze the influence of the chemical bonding on the energy loss of swift protons in various oxygen compounds.

In particular, it was shown that the influence of the band gap in the low-energy stopping power is much smaller than expected from previous theoretical estimations, showing a proportionality of the stopping cross-section with velocity for proton beams, down to energies of about 2 keV [3,5]. These results have renewed the interest in formulating theoretical models that could describe the characteristics of the energy loss phenomenon in insulators on a wide range of energies, including the low and the intermediate energy range around the stopping power maximum.

* Corresponding author. Tel.: +34-65-909578; fax: +34-65-903464.

E-mail address: ias@ua.es (I. Abril).

We propose a representation of the electronic energy-loss spectra of real solids (or its oscillator-strength distribution) based on Mermin-type dielectric functions $\epsilon_M(k, \omega)$ to describe the response of the outer electrons of the solid to an external perturbation [6–8]; $\hbar k$ and $\hbar\omega$ correspond, respectively, to the momentum and energy transferred to the target. The inner-shell electrons are described by an atomic model represented by the generalized oscillator strength (GOS) in the hydrogenic approach [9]. The energy-loss function (ELF) used in this model is adjusted in the optical limit (momentum transfer $\hbar k = 0$), using a set of experimental data for each particular element, and they are analytically extended to all values of wave number k through the properties of the Mermin dielectric function. This provides the complete energy-loss function $\text{Im}[-1/\epsilon(k, \omega)]$, which is consistent with the Kramers–Kronig relations and with the oscillator-strength sum rule for all values of k [7]. Since this description contains all the relevant information on the electronic transitions and band structure effects in the optical range, and a consistent extension to the whole (k, ω) range, it is expected that this model should provide a realistic description of the energy-loss spectra for each particular material. Within this scheme, we evaluate the electronic stopping cross-section and the energy-loss straggling of three oxides (Al_2O_3 , SiO_2 and ZrO_2) through the whole energy range of interest in relation with the experiments indicated above [1–3]. The nuclear stopping can be neglected in the range of energies we shall consider.

The stopping power S_p of a material, characterized by an energy loss function $\text{Im}[-1/\epsilon(k, \omega)]$, for a proton moving with velocity v through it, is obtained using the dielectric formalism as [10]

$$S_p(v) = \frac{2Z_1^2 e^2}{\pi v^2} \int_0^\infty \frac{dk}{k} \int_0^{kv} d\omega \omega \text{Im} \left[\frac{-1}{\epsilon(k, \omega)} \right], \quad (1)$$

where Z_1 is the projectile atomic number ($Z_1 = 1$ in the present case) and e is the elementary charge.

The energy-loss straggling $d\Omega^2/dx$ represents the fluctuation in the energy-loss spectrum, and it is given by [10]:

$$\frac{d\Omega^2}{dx}(v) = \frac{2Z_1^2 e^2 \hbar}{\pi v^2} \int_0^\infty \frac{dk}{k} \int_0^{kv} d\omega \omega^2 \text{Im} \left[\frac{-1}{\epsilon(k, \omega)} \right]. \quad (2)$$

The inelastic scattering that takes place in the solid with the outer electrons is complicated due to the effect of chemical bonding on the electron wave functions and by the existence of collective excitations; these interactions can be described in terms of a dielectric response function. We model the ω and k dependence of the ELF of a material by means of a linear combination of Mermin-type ELF, $\text{Im}(-1/\epsilon_M)$. In brief, the ELF is fitted to experimental data obtained in the optical limit, $k = 0$, and the electronic excitations of the outer shells are described by a sum of Mermin-type ELFs [6–8]:

$$\begin{aligned} & \text{Im} \left[\frac{-1}{\epsilon(k=0, \omega)} \right]_{\text{exper. (outer)}} \\ &= \sum_j A_j \text{Im} \left[\frac{-1}{\epsilon_M(k=0, \omega; \omega_j, \gamma_j)} \right]. \end{aligned} \quad (3)$$

The parameters A_j , ω_j and γ_j are related to the intensity, the position and the width, respectively, of the peaks and other structures observed in the energy-loss spectrum.

Inner-shell electrons have relatively large binding energies giving a strong binding to the nucleus and negligible collective effects. We describe the inner-shell excitations using a single-atom model through the GOS [9] in the hydrogenic approach that provides realistic values of the inner-shell ionization cross-sections, besides analytical expressions for K- and L-shell ionization [11].

The parameters used to fit the ELF are chosen in such a manner that: (i) a reasonably good fitting to the experimental ELF is obtained, and (ii) the effective number of electrons per molecule participating in electronic excitations up to a given energy $\hbar\omega$, namely

$$N_{\text{eff}}(\omega) = \frac{m}{2\pi^2 e^2 n} \int_0^\omega d\omega' \omega' \text{Im} \left[\frac{-1}{\epsilon(k, \omega')} \right], \quad (4)$$

tends to the number of electrons filling the orbitals of the target atoms, and, of course, to the total number of electrons of the molecule when the ex-

citation energy goes to infinity. Here n is the molecular density of the material and m is the electron mass.

The construction of the ELF requires the availability of the corresponding experimental data in a wide range of excitation energies; but for some elements and compounds these data are not always obtainable. For large $\hbar\omega$ the ELF of a compound A_yB_z can be constructed from the ELF of its elementary constituents, A and B, applying the weighted additivity of their respective ELF/ n ratios, where the ELF of each element is obtained from the X-ray scattering factors [12]; this proce-

dure is correct for energies comparable to that of the inner shells.

The left axes of Fig. 1(a–c) correspond to the ELF of the three materials discussed in this paper: Al_2O_3 , SiO_2 and ZrO_2 , respectively. For the lower energies, the experimental ELF was given directly by the existing data for each compound (represented by symbols, as indicated in the figure caption), whereas for the higher energies, where experimental data are not available, we use the ELF of the compound obtained applying the weighted additivity of the ELF/ n of the constituents. Our fitting is depicted as a solid line and the

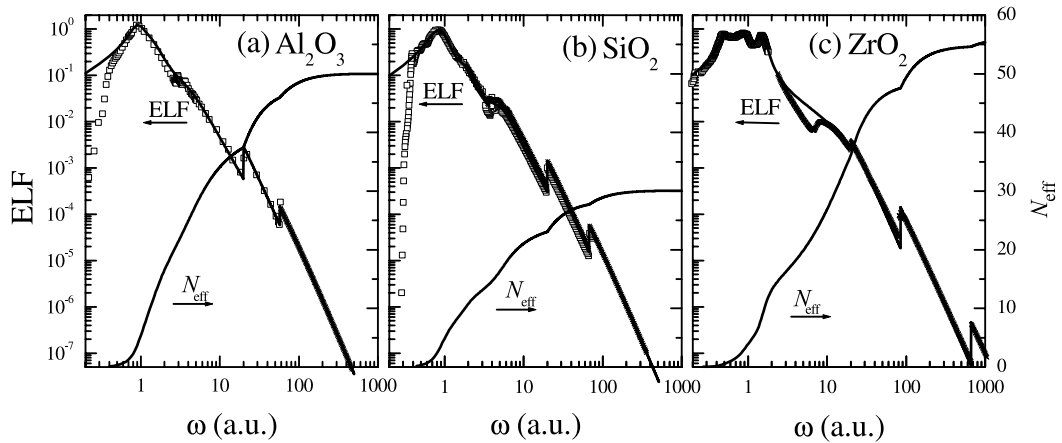


Fig. 1. ELF (left axes) and effective number of electrons (right axes) of three different oxides as a function of the excitation energy. The thick solid line represents our fitting to the experimental ELF and the experimental data are denoted by symbols: (a) Al_2O_3 , data from Hagemann et al. [13] (\square), (b) SiO_2 , data from Philipp [14] (\square) and Powell [15] (\blackstar), and (c) ZrO_2 , data from Frandon et al. [16] (\square).

Table 1
Parameters used to fit, through Eq. (3), the optical ELF of Al_2O_3 , SiO_2 and ZrO_2

Target	j	$\hbar\omega_j$ (eV)	$\hbar\gamma_j$ (eV)	A_j
Al_2O_3 ($\rho = 3.97 \text{ g/cm}^3$)	1	25.31	12.25	3.82×10^{-1}
	2	35.37	32.65	4.44×10^{-1}
	3	100.68	136.05	5.11×10^{-2}
SiO_2 ($\rho = 2.32 \text{ g/cm}^3$)	1	24.16	15.78	5.96×10^{-1}
	2	48.98	27.21	4.63×10^{-2}
	3	136.05	125.17	1.6×10^{-2}
ZrO_2 ($\rho = 5.6 \text{ g/cm}^3$)	1	13.06	2.72	8.03×10^{-2}
	2	16.87	8.16	1.69×10^{-1}
	3	24.49	10.07	2.35×10^{-1}
	4	41.36	15.97	2.16×10^{-1}
	5	108.84	498.78	1.28×10^{-1}

parameters used when fitting the contribution of the external electrons to the ELF appear in Table 1. We can see that there is a good agreement between the higher-energy part of the directly available ELF and the low-energy side of the calculated one. We notice also that the electrons of each atom that do not participate in the chemical bonding clearly become apparent as sharp edges in the ELF, whereas some otherwise sharp edges corresponding to atomic electrons now appear broadened due to their participation in the chemical bonding.

The right axes of Fig. 1(a–c) correspond to the effective number of electrons per molecule that participate in electronic excitations at a given energy, Eq. (4). It can be seen how the inner-shell electrons of the atomic constituents of each molecule progressively contribute to N_{eff} as the excitation energy $\hbar\omega$ increases, and they tend to the total number of electrons per molecule when $\hbar\omega \rightarrow \infty$.

An additional checking of our fitting procedure is obtained calculating the mean excitation energy I of each compound, that only depends on the electronic structure of the target [17]:

$$\ln I = \frac{\int_0^\infty d\omega \omega \ln \omega \operatorname{Im} \left[\frac{-1}{\epsilon(k, \omega)} \right]}{\int_0^\infty d\omega \omega \operatorname{Im} \left[\frac{-1}{\epsilon(k, \omega)} \right]}. \quad (5)$$

We obtain the following results: $I(\text{Al}_2\text{O}_3) = 145.3$ eV, $I(\text{SiO}_2) = 137$ eV and $I(\text{ZrO}_2) = 312.8$ eV,

which agree satisfactorily well with the available experimental mean ionization energy [18] $I^{\text{exp}}(\text{Al}_2\text{O}_3) = 145.2$ eV and $I^{\text{exp}}(\text{SiO}_2) = 139.2$ eV; unfortunately there is no experimental data for ZrO_2 . The application of Bragg's rule [19] to the mean ionization energy for these oxides gives the following values: $I^{\text{Bragg}}(\text{Al}_2\text{O}_3) = 143$ eV, $I^{\text{Bragg}}(\text{SiO}_2) = 141$ eV and $I^{\text{Bragg}}(\text{ZrO}_2) = 295$ eV.

Using the previous representations of the ELF for Al_2O_3 , SiO_2 and ZrO_2 , we have calculated their corresponding stopping power and energy-loss straggling for protons by integrating their oscillator-strength distributions over the k - ω plane, as indicated by Eqs. (1) and (2), respectively. The stopping cross-sections of Al_2O_3 , SiO_2 and ZrO_2 for protons are shown as solid lines in Fig. 2; available experimental data [1,3,20,21] are indicated by symbols. The main contribution to the stopping cross-sections are due to the excitations of the outer electrons, although the oxygen K-shell electrons have a contribution of $\sim 3\%$ when the proton energy is ~ 600 keV, increasing until 10% when the energy is 2500 keV. For comparison, we have also plotted as dashed lines the semiempirical predictions of SRIM [22]. The calculations performed with the present model are found in satisfactory agreement with the experimental results for the whole range of proton energies. The major deviations of our results with respect to SRIM appear at energies around and lower than that

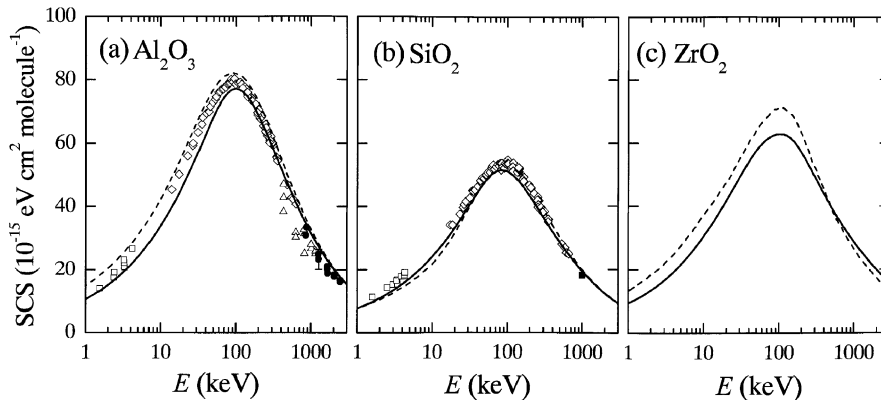


Fig. 2. Stopping cross-sections of (a) Al_2O_3 , (b) SiO_2 , and (c) ZrO_2 , as a function of the proton energy. For each case, the solid line represents our calculation, the dashed line is the prediction of SRIM [22], and the symbols refer to experimental data for protons (\diamond) [1], (\square) [3], (\bullet) [20], (full square) [21] and deuterons (\triangle) [20].

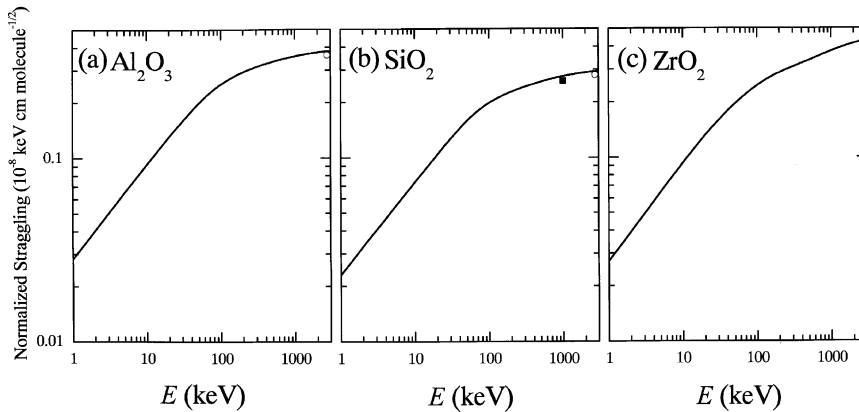


Fig. 3. Normalized energy-loss straggling $(\frac{1}{n} \frac{d\Omega_B^2}{dx})^{1/2}$ of (a) Al_2O_3 , (b) SiO_2 and (c) ZrO_2 , as a function of the proton energy. For each case, the solid line represents our calculation, and the symbols refer to experimental data ((full square) [21]) and (O) the adapted Bragg's rule for the Bohr energy-loss straggling.

corresponding to the maximum stopping cross-section; this is expected due to the increasing contribution of valence electrons to the stopping power at low energies, which is not properly taken into account by Bragg's rule. In particular, there are sizeable differences at low and intermediate energies for the case of ZrO_2 ; the need of experimental values in this case is evident, in order to clarify this discrepancy.

In Fig. 3 we show the normalized energy-loss straggling, $(\frac{1}{n} \frac{d\Omega_B^2}{dx})^{1/2}$, of Al_2O_3 , SiO_2 and ZrO_2 as a function of the proton energy. We compare our calculations with the experimental data of SiO_2 obtained by Kido [21] using nuclear resonance reactions. Adapting Bragg's rule to evaluate the Bohr energy-loss straggling, $d\Omega_B^2/dx$, of a compound A_yB_z as the weighted additivity of their respective elements, i.e. their $(d\Omega_B^2/dx)/n$ ratios, we obtain the values indicated by empty circles in Fig. 3, which should be considered as high energy limits. Nevertheless, our calculations derived from a proper description of valence and inner-shell electrons show that the adapted Bohr energy-loss straggling underestimates our more elaborate calculations in a 5–10%.

In summary, we have presented a theoretical model to describe the interaction and energy-loss parameters for protons penetrating three oxides. The model is based on Mermin-type dielectric

functions and reproduces very well the energy loss and straggling values through a wide energy range (2 keV–3 MeV) in all the cases where experimental data exists. No band gap effects are obtained at low energies, down to about 2 keV, in agreement with the reported experimental results of Ref. [3]. The parameters of the present model are tabulated to facilitate further applications. The model could be applied in energy-loss calculations or simulation studies, as well as in electron-mean-free-path or electron spectroscopy studies.

Acknowledgements

We thank G. Lantschner and H. Eckardt for useful discussions. This work was supported by the Spanish Comisión Interministerial de Ciencia y Tecnología (projects 1FD97-1358-C02-01, BFM2000-1050-C02-01 and BFM2000-1050-C02-02) and the Argentinian FONCYT (project PICT 0303579).

References

- [1] P. Bauer, W. Rössler, P. Mertens, Nucl. Instr. and Meth. Phys. Res. B 69 (1992) 46.
- [2] P. Bauer, R. Golser, F. Aumayr, D. Semrad, A. Arnau, E. Zarate, R. Diez-Muñoz, Nucl. Instr. and Meth. Phys. Res. B 125 (1997) 102.

- [3] K. Eder, D. Semrad, P. Bauer, R. Golser, P. Maier-Komor, F. Aumayr, M. Peñalba, A. Arnau, J.M. Ugalde, P.M. Echenique, *Phys. Rev. Lett.* 79 (1997) 4112.
- [4] P. Bauer, R. Golser, D. Semrad, P. Maier-Komor, F. Aumayr, A. Arnau, *Nucl. Instr. and Meth. Phys. Res. B* 136–138 (1998) 103.
- [5] J.I. Juaristi, C. Auth, H. Winter, A. Arnau, K. Eder, D. Semrad, F. Aumayr, P. Bauer, P.M. Echenique, *Phys. Rev. Lett.* 84 (2000) 2124.
- [6] I. Abril, R. Garcia-Molina, N.R. Arista, *Nucl. Instr. and Meth. Phys. Res. B* 90 (1994) 72.
- [7] D.J. Planes, R. Garcia-Molina, I. Abril, N.R. Arista, *J. Electron Spectrosc. Relat. Phenom.* 82 (1996) 23.
- [8] I. Abril, R. Garcia-Molina, C.D. Denton, F.J. Pérez-Pérez, N.R. Arista, *Phys. Rev. A* 58 (1998) 357.
- [9] H. Bethe, *Ann. Phys.* 5 (1930) 325.
- [10] J. Lindhard, *Mat.-Fys. Medd. K. Dan. Vidensk. Selsk.* 28 (8) (1954).
- [11] R.F. Egerton, *Electron Energy-Loss Spectroscopy in the Electron Microscope*, Plenum Press, New York, 1989.
- [12] B.L. Henke, E.M. Gullikson, J.C. Davis, *At. Data Nucl. Data Tables* 54 (1993) 2.
The ASCII files for the f_1 and f_2 scattering factors of the different elements can be obtained from <http://xray.uu.se/hypertext/henke.html>.
- [13] H.-J. Hagemann, E. Gudat, C. Kunz, Optical constants from the far infrared to the X-ray region: Mg, Al, Cu, Ag, Au, Bi, C and Al_2O_3 , Deutsches Elektronen-Synchrotron Report DESY SR-74/7, Hamburg, 1974, Unpublished; *J. Opt. Soc. Am.* 65 (1975) 742.
- [14] H.R. Philipp, in: E.D. Palik (Ed.), *Handbook of Optical Constants of Solids*, Vol. I, Academic Press, Orlando, 1985, p. 749.
- [15] C.J. Powell, in: E.D. Palik (Ed.), *Handbook of Optical Constants of Solids*, Vol. I, Academic Press, Orlando, 1985.
- [16] J. Frandon, B. Brousseau, F. Pradal, *Phys. Stat. Sol. (b)* 98 (1980) 379.
- [17] E. Shiles, T. Sasaki, M. Inokuti, D.Y. Smith, *Phys. Rev. B* 22 (1980) 1612.
- [18] ICRU Report 49, Stopping powers and ranges for protons and alpha particles, International Commission for Radiation Units and Measurements, Bethesda, 1992.
- [19] W.H. Bragg, R. Kleeman, *Philos. Mag.* 10 (1905) 318.
- [20] D.C. Turner, N.F. Mangelson, L.B. Rees, *Nucl. Instr. and Meth. Phys. Res. B* 103 (1995) 28.
- [21] Y. Kido, *Nucl. Instr. and Meth. Phys. Res. B* 24/25 (1987) 347.
- [22] J.F. Ziegler, SRIM. The stopping and range of ions in matter, Version 96.01.